

Developing an image-based, features recognition algorithm to determine optimal treatment for cervical cancer in low and middle income countries

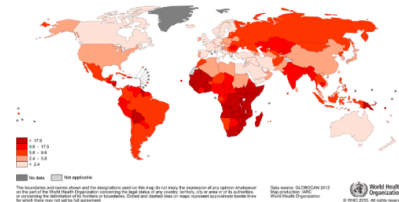
Keerat Singh

Abstract—Cervical cancer has become a problem for most third world countries because of their inability to determine the appropriate method of treatment which can vary depending on patients physiological differences. Health providers don't have the skills to identify which treatment will prevent the cancer; this is not only costly but it can even worsen the patient's condition. Certain treatments that work for some women can obscure future cancer growth in others. By first knowing the type of a woman's cervix, doctors should be able to treat the cancer accordingly. The goal of this research is to create an image classifier that will be able to determine the type of a woman's cervix, and therefore the appropriate treatment. The cervixes within the training and testing images are all considered non-cancerous, but they all showcase the individual transformation zone locations, which ultimately determine the different cervix types. The raw images will be fed into a Convolutional Neural Network (CNN) comprised of a combination of four layers. The first two alternating layers will essentially multiply feature weights, in the form of matrices, to individual pixels of the image, creating feature maps. These feature maps will then be reduced to vectors in the next layer, and then will be inputted into a sigmoid function to output the class of the image as either type 1, type 2, or type 3.

I. INTRODUCTION

Cervical cancer is a disease in which cells along the inner-lining of the lower uterus undergo pre-cancerous changes such as neoplasia and dysplasia (Peirson, Fitzpatrick-Lewis, Ciliska, Warren, 2013). Cervical cancer is mainly caused by an infectious agent, Human Papilloma Virus (HPV). The two variations, HPV 16 and HPV 18, occur through unprotected sex, and cause over 70% of all cervical cancer cases (Cervical Cancer, 2016). All sexually-active women have increased chances of obtaining high risk HPV types, thus leading to increased chances for pre-cancerous cell changes. Other risk factors include smoking tobacco, experiencing past history with cancer, and taking the contraceptive pill.

Approximately 500,000 women per year are diagnosed with cervical cancer globally, and 275,000 of those patients die of the disease (Wieringa, Zee, Vries, Vugt, 2016). The U.S. accounts for a very small percentage of that number (Siegel, Miller, Jemal, 2015). From 1930 to 2011, cervical cancer mortality rates in the US have decreased over 80% due to medical advances. In low and middle income countries (LMIC), the rates have only reduced 6% from 1930 to 2011. As illustrated on the map below, developing countries such as Kenya, Ethiopia, and Bolivia have much higher mortality rates than developed countries, such as the U.S. and Canada.



are about 60% lower than that of the U.S, leading to the need for more advanced and costly treatments downstream (Catarino, 2015).

To solve this problem, the majority of current research is focused on the analysis and implementation of more efficient screening programs in LMIC countries (Denny et al., 2017). Due to the relatively low medical experience of the practitioners, there have been numerous research projects that have looked into basic but equally-effective diagnosis techniques (Lee, Kang, Ju, 2016). For example, a large topic has been the use of acetic acid for a visual inspection test against the presence of HPV (Denny et al., 2017). Research has also been done with the replacement of acetic acid with Lugols iodine (Vyas, Bhalodia, Thakor, 2016). Both visual inspection techniques have had much more success in middle-income countries, such as parts of India and Pakistan. A large percentage of screening programs that are currently being looked into for LMIC countries are not feasible; despite being reliable in terms of accuracy, they require complex human and financial infrastructures to be implemented and maintained (Lee, Kang, Ju, 2016). In Sub-Saharan Africa alone, it was reported in 2016 that less than 5% of at-risk women had been screened, indicating new screening programs lack of implementation and success (Catarino, 2015). As a result, most cases of cervical cancer become invasive to the point that they are unable to treat. Many women in these parts of the world are receiving treatments that are ineffective and many times harmful to them (Intel MobileODT, 2017). Health providers often do not have the necessary skills, and more importantly, diagnostic resources, to recognize which treatments to use to prevent the spread of the cancer. The inability to discern which treatment will work for a woman based on her type of cervix has led to increased mortality, unnecessary expenses and the wastage of materials. False treatments and the lack of effective screening programs are substantial reason why most cases of cervical cancer in LMIC countries reach stage III and above, usually resulting in death (Denny et al., 2017). The goal of this research is to create an image classifier that will be able to determine the type of a woman's cervix, and therefore the appropriate treatment. The three cervical types are indicated below.

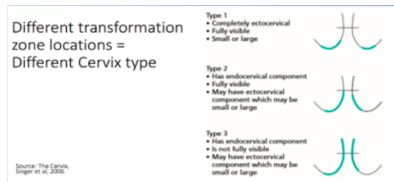


Fig. 2. Description of three types of cervixes

As a woman ages, the original squamo-columnar junction (SCJ), which is the boundary between two different types of epithelial cells, gets transformed into a new SCJ by processes of metaplasia. As one can see below, the area between the new SCJ and original SCJ is called the transformation zone.

The difference in transformation zones defines the three types of cervixes.

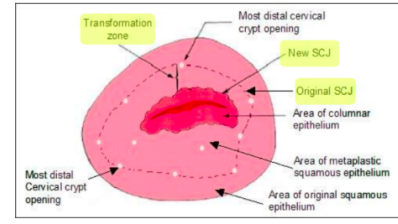


Fig. 3. Anatomy of cervix

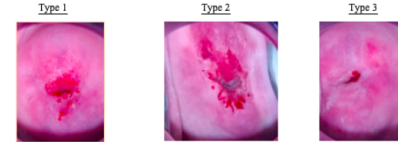


Fig. 4. Examples of three types from data

As one can see in figure 4, it is not easy for inexperienced doctors to distinguish between these three types based on simply looking at the pictures. Therefore, an automatic classification system would be particularly useful to solve this problem.

II. METHODS

The model was intended to be based on figure 5. For each

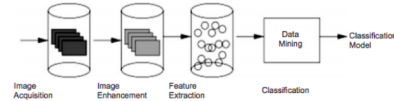


Fig. 5. Classification system

the image enhancement step, there were multiple approaches that were attempted. This was because there was trouble in standardizing the original training set to be passed through a neural network. The training set was composed of 248 type 1 images, 780 type 2 images, and 450 type 3 images making for a total of 1478 images. The images varied in size, as the smallest images were 240x280 pixels and the largest were 2048x2096 pixels. Theoretically, the images should have its center aligned with the center of the cervix. But, in reality there was great variation within the data in where the center was with respect to the image. The methods I attempted to fix these problems were histogram equalization, zero-padding, and cropping a region of interest. While these will be mentioned briefly, the final system was simply a convolutional neural network.

A. Histogram Equalization

A variation of histogram equalization was used in an attempt to increase image contrast and enhance differences within the center of the cervix. The algorithm works by finding the average number of pixels, p_n , with an intensity n , where n includes each integer from 0 to 255. Then, it fits the values of p_n to a normal curve, and accordingly adjusts the intensities of the image.

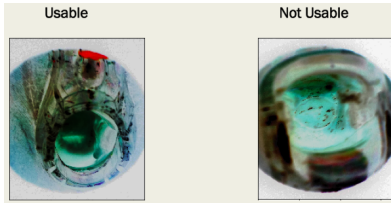


Fig. 6. Usable and not usable outputs from histogram equalization

As shown in figure 6, while some modified images were usable in that the center was enhanced, others were not usable due to increased contrast in parts of the image other than the center.

B. Zero-padding

Zero-padding is the process of adding borders of black pixels to images in an attempt to attain one common size. Before images could be inputted into a neural network, they had to be standardized in terms of size. Since the original data set was composed of many different sizes, a zero-padding method was implemented. While it worked in terms of attaining a common size, the features of the cervix became much less noticeable due to the increase in image width and height. Also, since the final size was the largest width and height in the original data set, every image became much bigger. This, in turn, would make for a much less efficient network.

C. Cropping a region of interest

Still in an attempt to standardize the images, a method in which the region of interest was cropped and set as the input image was attempted. The original data set was problematic in that the region of interest within the cervix wasn't in the same position in all of the images and there wasn't a consistent size. By identifying and cropping a commonly-sized region of interest, both of these problems would be solved.



Fig. 7. Results from Crop-ROI method

As shown in figure 7, the implementation wasn't consistently identifying the region of interest. For some of the images, like the left-most image, the algorithm worked as expected, correctly isolating the center of the cervix. For other images, like the one in the middle, differences in lighting and shading caused the algorithm to include parts outside of the center region. Since the images were not all taken in the same fashion, many of the images were outputted with little to no isolation like the right-most image.

D. Convolutional Neural Network

To enhance the images, a method named *normalize_image_features* was used.

```
def normalize_image_features(paths):
    #Input: list of paths
    #Output: list of resized images that have been
            transposed for Conv2d layer
    imf_d = {}
    p = Pool(cpu_count())
    ret = p.map(get_im_cv2, paths)
    #ret holds a list: [[image path, resized image], ...]
    for i in range(len(ret)):
        imf_d[ret[i][0]] = ret[i][1]
        #imf_d[image path in ret] = resized image
    ret = []
    fdata = [imf_d[f] for f in paths]
    #fdata holds a list: [resized image, ...]
    fdata = np.array(fdata, dtype=np.uint8)
    #fdata is now a numpy array of ints
    fdata = fdata.transpose((0, 3, 1, 2))
    #Usually its (2, 0, 1) since it changes the
        image from (0, 1, 2)->(width, height,
        channel)
    #to (2, 0, 1)->(channel, width, height) for the
        Conv2d layer,
    #but since we have 4 dimensions, it gets bumped
        up one to (3, 1, 2);
    fdata = fdata.astype('float32')
    fdata = fdata / 255
    #fdata now has values between 0 and 1
    return fdata
```

In summary, *normalize_image_features* transposed the source image to allow for input into the initial layer of the classification network. At the beginning of the method, the original image was re-sized using the *get_im_cv2* method, as shown below.

```
def get_im_cv2(path):
    #Input: file path of image
    #Output: [original path, resized image]
    img = cv2.imread(path)
    resized = cv2.resize(img, (64, 64), cv2.
        INTER_LINEAR) #INTER_LINEAR is algorithm
    #to downsize image
```

The source image was downsized to 64 x 64 using *cv2.INTER_LINEAR*. The *INTER_LINEAR* algorithm bi-linearly interpolated specific sections of the image to be used in the re-sized image. In *normalize_image_features*, the file path of the original image was mapped to *get_im_cv2*, which re-sized it to be used for the rest of the method.

As shown in *normalize_image_features*, the original initialization of the variable *fdata* contained the source image with dimensions in the order [image.id, width, height, channel]. After the transpose method was used, *fdata* contained the image with dimensions in the order [image.id, channel, width, height]. This enhancement of the image was necessary for inputting the image into the first layer of the Convolutional Neural Network (CNN): the Conv2D layer. The specific library that built the Conv2D layer, keras, required that the channel, which specified that the image was of color, came before the width and height. Before *fdata* was outputted at the end of the function, it was scaled down by a factor of 255 to get a value between 0 and 1.

For the final steps of feature extraction and classification, an eight layer CNN was used as shown *create_model*.

```
def create_model(opt_='adamax'):
    model = Sequential()
    model.add(Convolution2D(4, 3, 3, activation='relu', dim_ordering='th',
                           input_shape=(3, 64, 64)))
    #Could try different input shape

    #Activation='relu' to discover nonlinear patterns of data
    #dim_ordering = 'th' to match (0, 3, 1, 2) images were transposed to
    #Four 3x3 filters
    model.add(MaxPooling2D(pool_size=(2, 2), strides=(2, 2), dim_ordering='th'))
    model.add(Convolution2D(8, 3, 3, activation='relu', dim_ordering='th'))
    model.add(MaxPooling2D(pool_size=(2, 2), strides=(2, 2), dim_ordering='th'))
    #model.add(Dropout(0.2))
    #model.add(Dropout(0.8))
    #model.add(Dropout(0.6))
    #model.add(Dropout(0.4))
    model.add(Dropout(0.1))
    #Sets a fraction of rate of input units to 0 to prevent overfitting
    model.add(Flatten())
    #Creates 1D feature vector for Dense layers
    model.add(Dense(12, activation='tanh')) #
    Classifies
    #model.add(Dropout(0.1))
    #model.add(Dropout(0.7))
    #model.add(Dropout(0.5))
    #model.add(Dropout(0.3))
    model.add(Dropout(0.05))
    model.add(Dense(3, activation='softmax')) #
    Classifies

    model.compile(optimizer=opt_, loss='sparse_categorical_crossentropy', metrics=['accuracy'])
    #Compiles all layers of model with optimizer, loss function, and metrics (to evaluate performance)
    return model
```

The first four layers, an alternating series of convolutional and max pooling layers, performed feature extraction on the inputted image. The convolutional layer performed the convolution operation with filters on sections of the image. The convolution operation was an element-wise product and sum of two arrays. Conceptually, if there was a feature of interest that could be detected by the filter, then it would be highlighted in the output of the convolutional layer.

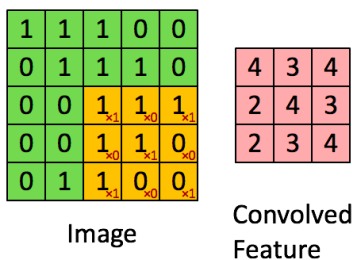


Fig. 8. Convolutional layer

The pooling layer then singled out where the feature detected was most prevalent. After multiple combinations of these layers, the network isolated each feature and its location within an image as shown in Figure 8. These feature maps were flattened into one-dimensional vectors in the flatten layer. Based on the parameters of the transferred vector, the final dense layer predicted the output of the image to be either type 1, type 2, or type 3.

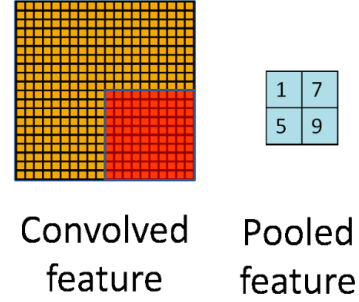


Fig. 9. Pooling layer

As shown in *create_model*, there were two dropout layers in the model architecture. The dropout rate established how many neurons in the next layer get deactivated. This forced the model to learn the same pattern through different neurons, thus preventing over-fitting. The model was tested with different dropout rates to see how they affected the final results.

III. RESULTS

Dropout Rate 1 \ Dropout Rate 2	Acc.	Loss
0.1, 0.05	0.8500	0.3718
0.2, 0.1	0.8269	0.44034
0.4, 0.3	0.7194	0.6529
0.6, 0.5	0.6139	0.8669
0.8, 0.7	0.5352	0.9804

TABLE I

CNN: TRAINING RESULTS WITH DIFFERENT DROPOUT PAIRS

IV. CONCLUSIONS

As shown in Table 1, this specific convolutional neural network architecture was able to achieve a relatively high accuracy with lower dropout rates. The rate of increase in accuracy with respect to the change in dropout rates is encouraging, as the lowest dropout pair returned an accuracy of 0.8500 and a loss of 0.3718, while the highest returned an accuracy of 0.5352 and a loss of 0.9801.

Even though future implementations of this model should have a lower dropout pair, one will have to beware of over-fitting. This occurs when the model becomes too accustomed to the patterns within the training data, and, therefore, fails at generalizing to the test data. Even though the results of the model improved with lower dropout rates, the chances for over-fitting also improved. Therefore, future models will

not contain dropout rates as low as the first pair in Table 1, rather they will have rates around the second pair.

Future work includes fine-tuning the Network's architecture to further improve accuracy and reduce the loss. These tests include: increasing the input distortion and experimenting with different interpolation algorithms from the OpenCV library.

Increasing the input distortion is a method used to prevent over-fitting. By transforming the training data through each epoch, the model learns patterns that can be generalized to a broader range of data. The rate at which the data are transformed is set in the *clean_images* function.

```
def cleanImages():
    datagen = ImageDataGenerator(rotation_range
                                =0.3, zoom_range=0.3)
    #rotation_range = random rotation of images up
    #to 0.3 degrees
    #zoom_range = random zoom of images up to a
    #scale of 0.3
    datagen.fit(train_data)
    return datagen
```

The current interpolation algorithm, *INTER_LINEAR*, is used to maximize the features that remain in the image after downsizing. This algorithm can be changed using OpenCV's many different options. By finding the best algorithm, the model will be better equipped to isolate and identify patterns.

REFERENCES

- [1] Catarino, R. (2015). Cervical cancer screening in developing countries at a crossroad: Emerging technologies and policy choices. *World Journal of Clinical Oncology*, 6(6), 281. doi:10.5306/wjco.v6.i6.281
- [2] Cervical cancer. (2016). Retrieved May 18, 2017, from <http://www.cancerresearchuk.org/aboutcancer/cervical-cancer/risks-causes>
- [3] Cervical Cancer Treatment. (2016). Retrieved May 18, 2017, from https://www.cancer.gov/types/cervical/patient/cervical-treatment-pdqsection/_180
- [4] Denny, L., Sanjose, S. D., Mutebi, M., Anderson, B. O., Kim, J., Jeronimo, J., . . . Sankaranarayanan, R. (2017). Interventions to close the divide for women with breast and cervical cancer between low-income and middle-income countries and high-income countries. *The Lancet*, 389(10071), 861-870. doi:10.1016/s0140-6736(16)31795-0
- [5] Intel MobileODT Cervical Cancer Screening. (2017.). Retrieved May 18, 2017, from <https://www.kaggle.com/c/intel-mobileodt-cervical-cancer-screening>
- [6] Lee, H., Kang, Y., Ju, W. (2016). Cervical Cancer Screening in Developing Countries: Using Visual Inspection Methods. *Clinical Journal of Oncology Nursing*, 20(1), 79-83. doi:10.1188/16.cjon.79-83
- [7] McKee, S. J., Bergot, A., Leggatt, G. R. (2015). Recent progress in vaccination against human papillomavirus-mediated cervical cancer. *Reviews in Medical Virology*, 25, 54-71. doi:10.1002/rmv.1824
- [8] Peirson, L., Fitzpatrick-Lewis, D., Ciliska, D., Warren, R. (2013). Screening for cervical cancer: a systematic review and meta-analysis. *Systematic Reviews*, 2(1). doi:10.1186/2046-4053-2-35
- [9] Sahasrabudhe, V. V., Parham, G. P., Mwanahamuntu, M. H., Vermund, S. H. (2011). Cervical Cancer Prevention in Low- and Middle-Income Countries: Feasible, Affordable, Essential. *Cancer Prevention Research*, 5(1), 11-17. doi:10.1158/1940-6207.capr-11-0540
- [10] Shulman, L. (2012). American Cancer Society, American Society for Colposcopy and Cervical Pathology, and American Society for Clinical Pathology Screening Guidelines for the Prevention and Early Detection of Cervical Cancer. *Yearbook of Obstetrics, Gynecology and Women's Health*, 2012, 339-342. doi:10.1016/j.yobg.2012.06.159
- [11] Siegel, R. L., Miller, K. D., Jemal, A. (2015). Cancer statistics, 2015. *CA: A Cancer Journal for Clinicians*, 65(1), 5-29. doi:10.3322/caac.21254
- [12] Vyas, K., Bhalodia, K., Thakor, N. (2016). Role of Pap's smear and visual inspection of cervix with Lugol's iodine for early detection of premalignant and malignant lesions of cervix: a cross sectional study. *International Journal of Reproduction, Contraception, Obstetrics and Gynecology*, 2684-2686. doi:10.18203/2320-1770.ijrcog20162646
- [13] Wieringa, H. W., Zee, A. G., Vries, E. G., Vugt, M. A. (2016). Breaking the DNA damage response to improve cervical cancer treatment. *Cancer Treatment Reviews*, 42, 30-40. doi:10.1016/j.ctrv.2015.11.008